

1 *Supplement of*

2

3 **Changing pattern of ice flow and mass balance for glaciers discharging into**
4 **the Larsen A and B embayments, Antarctic Peninsula, 2011 to 2016**

5

6 H. Rott et al.

7 *Correspondence to:* Helmut.Rott@enveo.at

8

9

10 **Contents**

11 **Section 1 – Overview on glacier basins for retrieval of volume change and mass balance**

12 The outlines of the glacier basins for retrieval of volume change and mass balance are
13 displayed on a Landsat image (Figures S1 and S2). Table S1 contains a list of the basins with
14 area extent in 2013 and 2016 and the GLIMS ID for the main glacier in each basin.

15 **Section 2 – Data coverage by TanDEM-X interferometric SAR data**

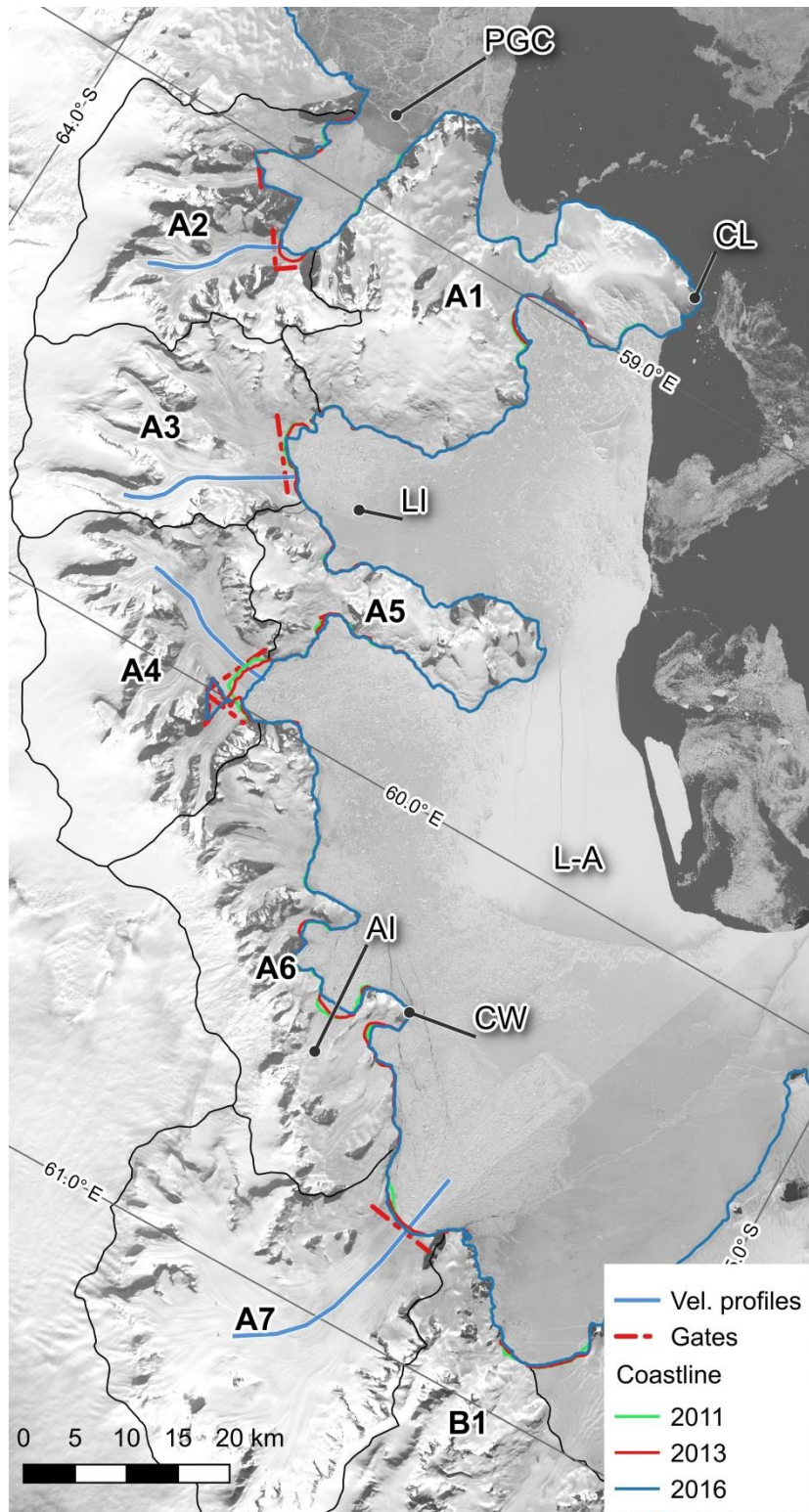
16 A map with area coverage of the TanDEM-X SAR image tracks used for DEM retrieval is
17 shown (Fig. S3) and the specifications of the DEMs used for generating surface elevation
18 change (SEC) products are listed (Table S2).

19 **Section 3 – Estimation of uncertainty for surface elevation change**

20 Details on the procedure and data base for estimating the uncertainty of the TanDEM-X maps
21 of surface elevation change are presented.

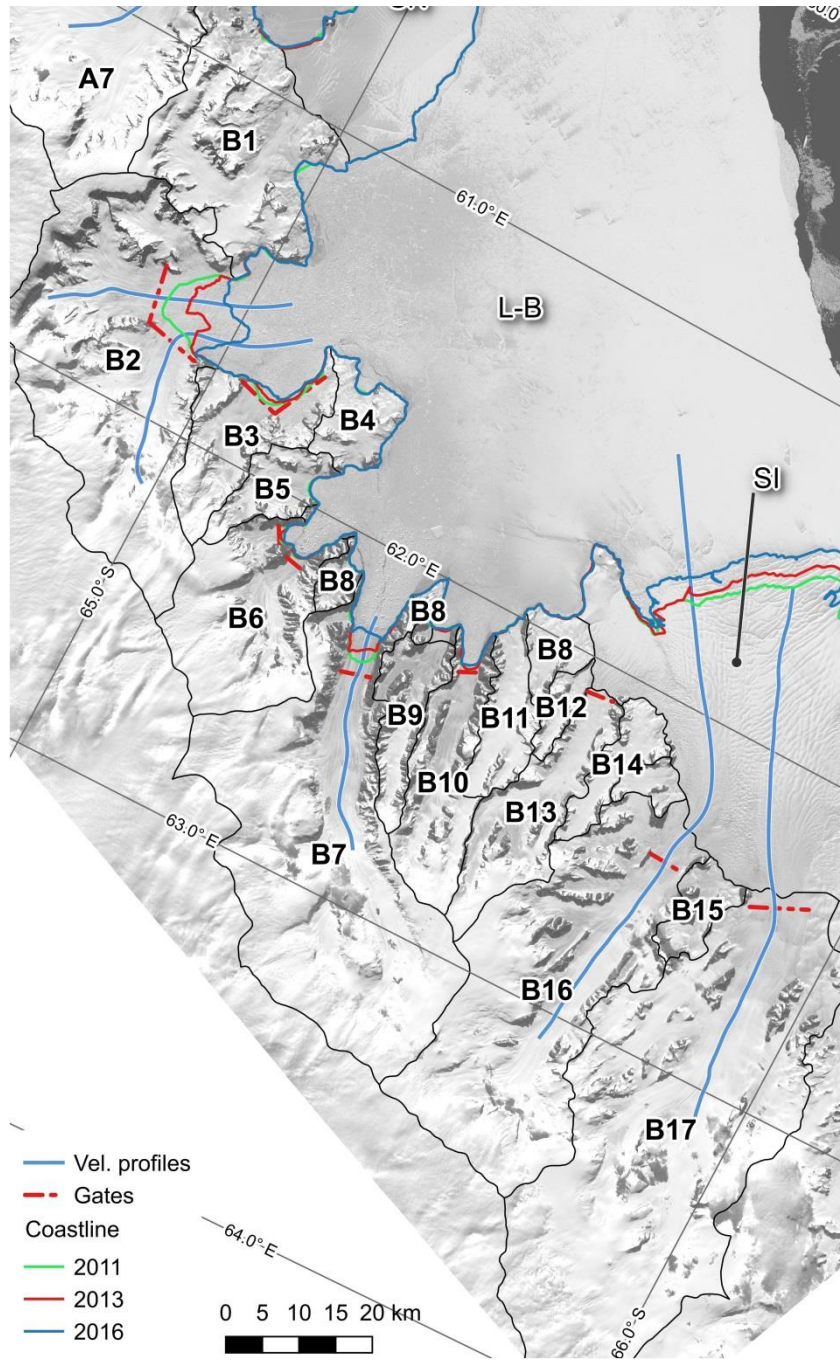
22

23



25

26 **Figure S1.** Outlines of glacier basins plotted on Landsat image of 2016-10-29. Coastlines
27 from TanDEM-X images mid-2011, -2013, -2016. AI -Arrol Icefall, CW – Cape Worsley, CL-
28 Cape Longing, L-A - Larsen A embayment, LI - Larsen Inlet, PGC – Prince Gustav Channel
29 Red broken lines: gates for calving fluxes. Blue lines: Ice velocity profiles.



30

31 **Figure S2.** Outlines of glacier basins plotted on Landsat image of 2016-10-29. Coastlines
 32 from TanDEM-X images mid-2011, -2013, -2016. L-B - Larsen B embayment, SI – SCAR
 33 Inlet ice shelf. Red broken lines: gates for calving fluxes. Blue lines: Ice velocity profiles.

34

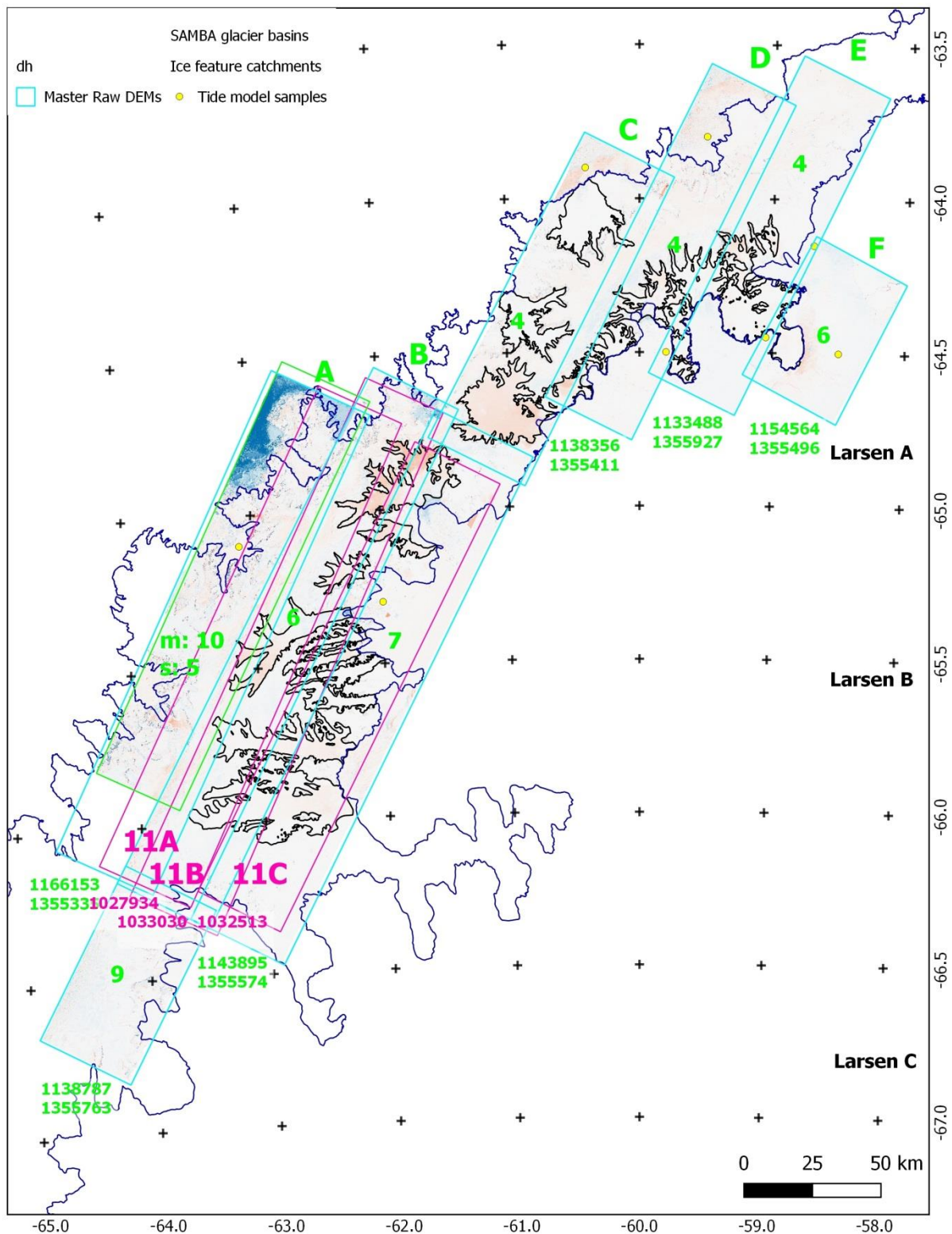
35 **Table S1.** Glacier catchments on northern Antarctic Peninsula (API) for retrieval of surface
 36 elevation change (SEC) and mass balance. Basin outlines inland are from the data set of Cook
 37 et al. (2014). The position of glacier fronts 2013 and 2016 are from geocoded TerraSAR-X
 38 images of June & July 2013 and July & August 2016.

Nr.	Glacier Basin Name	Area [km ²]		GLIMS ID Nr. (main glaciers of basin)
		2013	2016	
A1	Cape Longing Peninsula	667.30	668.91	G300465E64251S
A2	Sjørgen-Boydell, SB	525.47	527.55	G300700E64157S
A3	Albone, Pyke, Polaris, Eliason, APPE	511.29	513.58	G300465E64251S
A4	Dinsmoor, Bombardier- Edgeworth, DBE	646.50	653.93	G299838E64288S
A5	Sobral Peninsula	256.63	257.90	G300323E64397S
A6	Cape Worsley Coast	619.39	625.07	G299805E64456S
A7	Drygalski	998.54	998.32	G298872E64662
B1	Six glaciers west of Seal Nunataks	638.07	638.66	G298833E64908S
B2	Hektoria Green, HG	1167.49	1215.35	G298013E64919S
B3	Evans	266.92	272.32	G297915E65081S
B4	Evans Glacier Headland	117.66	117.66	G298295E65188S
B5	Punchbowl	119.94	119.88	AQ7LAB000009
B6	Jorum	460.33	461.41	G297567E65197S
B7	Crane	1322.57	1333.41	G297010E65410S
B8	3 small basins at Larsen B coast	142.64	142.64	G297840E65267S, G297936E65370S G297950E65543S
B9	Mapple	155.43	155.43	G297654E65415S
B10	Melville	291.47	292.91	G297326E65499S
B11	Pequod	150.35	150.58	G297685E65521S
B12	Rachel	51.80	51.80	G297822E65579S
B13	Starbuck	299.38	299.38	G297312E65606S
B14	Stubb	108.34	108.34	G297847E65684S
B15	2 small basins draining to SCAR Inlet ice shelf	136.78	136.78	G297762E65716S G297484E65849S
B16	Flask	1130.58	1130.58	G296666E65721S
B17	Leppard	1851.02	1851.02	G297153E65938S

40 **Section 2 – Data coverage by TanDEM-X interferometric SAR data**

41 **Table S2.** Raw DEMs processed as basis for generating SEC products. B6 and B9,
 42 respectively C4 and C7, include sequential sections of the same swath. Date refers to image
 43 acquisition. HoA is height of ambiguity. All images are descending equator crossing / right
 44 looking. Incidence angle refers to mid-swath. For spatial coverage see Fig. S.3.

Scene Label	Master / Slave	Date	HoA [m]	Rel. Orbit	Incidence. Angle
A	M	2013-10-02	-174.08	34	38.4
B6	M	2013-07-01	-60.64	125	45.6
B9	M	2013-07-01	-60.64	125	45.6
C4	M	2013-06-20	-56.73	125	40.6
C7	M	2013-06-20	-56.73	125	40.6
D	M	2013-06-09	-53.31	125	38.4
E	M	2013-05-18	-52.23	125	36.1
F	M	2013-07-29	-68.93	49	40.6
A	S	2016-07-10	-27.65	34	38.4
B6	S	2016-08-07	-26.64	125	45.6
B9	S	2016-08-07	-26.64	125	45.6
C4	S	2016-07-27	-29.11	125	40.6
C7	S	2016-07-27	-29.11	125	40.6
D	S	2016-07-16	-27.55	125	38.4
E	S	2016-08-18	-20.62	125	36.1
F	S	2016-07-22	-29.69	49	40.6
11A	S	2011-05-06	-50.59	34	37.3
11B	S	2011-06-30	51.80	34	36.1
11C	S	2011-06-25	57.62	125	41.0



46

47 **Figure S3.** Geographic coverage of TanDEM-X tracks for generating DEMs and maps of
 48 surface elevation change. Red: tracks for 2011 DEMs. Green: tracks for 2013 to 2016 DEMs.

49 Data specifications in Table S2.

50

51

52 **Section 3 – Estimation of uncertainty for surface elevation change**

53 For estimating the uncertainty of the TanDEM-X (TDM) elevation change product we
 54 compare TDM SEC data over the time span 2011 to 2016 with surface elevation rate of
 55 change data (dh/dt, product code IDHDT4) derived from Airborne Topographic Mapper
 56 (ATM) swathes, acquired during NASA IceBridge campaigns on 2011-11-14 and 2016-11-10
 57 (Studinger, 2014, updated 2017). Each IDHDT4 data record corresponds to an area where two
 58 ATM lidar swathes have co-located measurements. The IDHDT4 data are provided as discrete
 59 points representing 250 m x 250 m surface area and are posted at about 80 m along-track
 60 spacing. We compare mean values of cells comprising 7 x 7 TDM dh/dt pixels (of about 12 m
 61 x 12 m pixel size) with the corresponding IDHDT4 points along flowlines of six glaciers
 62 (Table S3). The ATM profiles extend from the ice front (on Leppard Glacier from a position
 63 several km up-glacier) up to different altitudes. On Drygalski Glacier and Crane Glacier we
 64 start the comparison several km inland of the front, because the lower sections of the terminus
 65 are very crevassed and the ice front positions differed on the dates of the ATM and TDM
 66 DEM acquisitions. A small percentage of the ATM dh/dt data shows high RMS (in crevasse
 67 zones and on steep slopes); these points are not used for the comparison.

68 **Table S3.** Mean rates of elevation change (dh/dt) 2011 to 2016 measured by ATM and
 69 TanDEM-X (TDM) for longitudinal profiles on Larsen outlet glaciers. $\Delta\langle dh/dt \rangle$ - difference of
 70 mean dh/dt (ATM – TDM.) RMSD – root mean square difference.

Glacier	dh/dt [m a ⁻¹] ATM 2011-16	dh/dt [m a ⁻¹] TDM 2011-16	$\Delta\langle dh/dt \rangle$ [m a ⁻¹]	RMSD [m a ⁻¹]	Nr. ATM samples
Crane	-2.460	-2.472	+0.012	0.219	238
Flask	-1.346	-1.272	-0.074	0.149	172
Leppard	-1.092	-0.896	-0.196	0.218	205
Melville	-1.362	-1.299	-0.063	0.232	165
Starbuck	-0.459	-0.309	-0.156	0.172	41
Drygalski	-4.707	-4.663	-0.044	0.350	92

71 For the error analysis we assume that the differences result from uncertainties in both data
 72 sets. We assume for RMSD = 0.28 m a⁻¹ (as representative value), resulting in RMSE = 0.20
 73 m a⁻¹ at the scale of individual cells for the each of the two data sets. This number is valid for
 74 a dh/dt time span of 1 year, derived from Δh measurements over a time span of 5 years.
 75 Measurements for the shorter periods (2 years, 3 years) are scaled accordingly. In addition, we
 76 include uncertainty estimates for a possible bias, with bulk values for the mapped area below
 77 the escarpment, the unsurveyed slopes, and the ice plateau.

78 The following formulation is applied for estimating the uncertainty of volume change, $E_{\Delta V}$
79 [$\text{m}^3 \text{a}^{-1}$], for a glacier basin covering an area A_B :

$$E_{\Delta V} = A_B \sqrt{f_m \frac{S_e^2}{n} + f_m E_m^2 + f_p E_p^2}$$

80 The following values are used to obtain annual rates of volume change for the Larsen glacier
81 basins, based on Δh measurements over time spans of 2 years (2011-2013) and 3 years (2013-
82 2016):

- 83 • S_e , random error for the TDM dh/dt map: $S_e = 0.58 \text{ m a}^{-1}$ (Δh 2 yr); $S_e = 0.39 \text{ m a}^{-1}$ (Δh
84 3 yr)
- 85 • E_m , possible bias for TDM dh/dt maps below the escarpment: $E_m = 0.075 \text{ m a}^{-1}$ (Δh 2
86 yr); $E_m = 0.05 \text{ m a}^{-1}$ (Δh 3 yr)
- 87 • E_p , possible bias for dh/dt on ice plateau and on unsurveyed slopes: $E_p = 0.15 \text{ m a}^{-1}$
88 (Δh 2 yr); $E_p = 0.10 \text{ m a}^{-1}$ (Δh 3 yr)

89 For the first term under the square-root an estimate for the number of statistically independent
90 samples (n) is needed, accounting for spatial correlation. We assume a distance of 500 m for
91 spatial decorrelation. The second term accounts for a possible bias of the TDM dh/dt maps
92 below the escarpment. The factors f_m and f_p account for the extent of the respective area
93 relative to the total basin area. For converting volume change to mass change we assume a
94 mean density $\rho = 900 \text{ kg m}^{-3}$. For estimating the uncertainty of sub-regions (Larsen A, Larsen
95 B embayment, SCAR Inlet) we assume that the errors for glaciers covered by a single TDM
96 track are correlated (the errors are added) and the errors of different tracks are uncorrelated.

97

98 **References**

99 Studinger, M. S: IceBridge ATM L4 Surface Elevation Rate of Change, Version 1, Subset
100 M699, S10, Boulder, Colorado USA. NASA National Snow and Ice Data Center Distributed
101 Active Archive Center, doi: <http://dx.doi.org/10.5067/BCW6CI3TXOCY>, [Accessed 25 July
102 2017], 2014, updated 2017.

103